Analytic approximation with real constraints, with applications to inverse diffusion problems

J. Leblond, J.-P. Marmorat, and J. R. Partington

Abstract. The methods of constrained approximation in Hilbert spaces of analytic functions are applied to the solution of the inverse problems of detecting cracks or sources in a two-dimensional material by means of boundary measurements. Issues of well-posedness are discussed, and results on continuity and robustness with respect to the given data are established. Constructive and efficient methods for resolution of the above approximation problems are presented. The techniques are illustrated by numerical examples incorporating a further rational approximation step.

Key words. Approximation, extremal problems, analytic functions, Hardy spaces, Toeplitz and Hankel operators, inverse problems.

AMS classification. 41A29, 35R30, 31A25, 47A57.

1. Introduction

1.1. Notation

By H^2 we denote the Hardy space on the unit disc $\mathbb{D}$, and by $\overline{H}^2$ the set of functions $\overline{f}$ for $f \in H^2$, where $\overline{f}(z) = \overline{f(1/\bar{z})}$. It is well-known that H^2 may be embedded isometrically as a closed subspace of $L^2(\mathbb{T})$, for $\mathbb{T}$ the unit circle.

The orthogonal complement of H^2 in $L^2(\mathbb{T})$ is written as $\overline{H}_0^2$; it coincides with the subset of $\overline{H}^2$ consisting of functions that vanish at infinity. We write P for the orthogonal projection $P : L^2(\mathbb{T}) \to H^2$ and similarly $\overline{P}$ for the orthogonal projection $\overline{P} : L^2(\mathbb{T}) \to \overline{H}^2$.

Likewise, H^∞ denotes the Hardy space of bounded analytic functions in $\mathbb{D}$, which may be regarded as a closed subspace of $L^\infty(\mathbb{T})$ in a natural way, while $A(\mathbb{D}) \subset H^\infty$ denotes the disk algebra consisting of analytic functions with continuous boundary values. See [15] for more details on Hardy spaces.

Let I be a compact subset of the unit circle $\mathbb{T} \subset \mathbb{C}$ such that I and $J = \mathbb{T} \setminus I$ have positive Lebesgue measure. The usual inner product in $L^2(\mathbb{T})$ is denoted by $\langle f, g \rangle$ for $f, g \in L^2(\mathbb{T})$, the associated norms on $L^2(\mathbb{T})$ and $L^2(I)$ are written as $\| \cdot \|$ and $\| \cdot \|_I$, respectively, while $\| \cdot \|_J^2 = \| \cdot \|^2 - \| \cdot \|_I^2$ on $L^2(J)$. Whenever f_1 is defined on I and f_2 on J, we write $f_1 \vee f_2$ for the function equal to f_1 on I and f_2 on J.

Let E be a subset of $\mathbb{T}$ with positive measure. The space of real-valued L^2 functions on E is denoted by $L_{\mathbb{R}}^2(E)$. We also write χ_E for the characteristic function of E. We recall that the modulus of continuity of a function $f \in C(E)$ is defined by

$$\omega_f(\delta) = \sup \{|f(x) - f(y)| : x, y \in E, \ |x - y| \le \delta\}.$$

For $0 < \alpha < 1$ the Lipschitz (or Hölder–Zygmund class) is defined by

$$C^\alpha(E) = \{f \in C(E) : \omega_f(\delta) = O(\delta^\alpha)\},$$

with norm

$$\|f\|_\alpha = \|f\|_{L^\infty(E)} + \sup_{\delta > 0} \frac{\omega_f(\delta)}{\delta^\alpha}.$$

To relate the real and imaginary parts of an analytic function, we shall make use of the *Hilbert transform* (or *harmonic conjugation*), of which the basic properties can be found in [3, pp. 104–106]. Let u be a function in $L^2_\mathbb{R}(\mathbb{T})$; then the Hilbert transform of u is the unique function v in $L^2_\mathbb{R}(\mathbb{T})$ with vanishing Fourier coefficient $\hat{v}(0) = 0$ such that $u + iv$ has a holomorphic extension to the disc. The Hilbert transform is a contraction in the L^2 norm.

1.2. Physical motivation: inverse diffusion problems

Methods of constrained approximation have been used before in the solution of various inverse problems for PDEs, and we refer to the survey [13] for an introduction to this topic in other contexts.

Cracks

Consider the inverse geometrical problem of detecting and locating cracks, modelled by C^2 simple curves σ, inside a 2 dimensional material by means of boundary measurements. These can consist of either thermal, electrical, or acoustic data, depending on the experimental framework. Without loss of generality, using conformal mapping, we can handle this issue in the unit disc $\mathbb{D} \supset \sigma$, where it can be written as [1, 10]:

$$\begin{cases} \Delta u = 0 & \text{in} \quad \mathbb{D} \setminus \sigma, \\[2mm] \dfrac{\partial u}{\partial n} = 0 & \text{on} \quad \sigma, \\[2mm] \dfrac{\partial u}{\partial n} = \Phi & \text{on} \quad \mathbb{T}, \end{cases} \tag{1.1}$$

for a flux $\Phi \in L^2_\mathbb{R}(\mathbb{T})$ which satisfies

$$\int_\mathbb{T} \Phi \, d\theta = 0, \tag{1.2}$$

and with the normalisation condition

$$\int_\mathbb{T} u \, d\theta = 0.$$

From additional *incomplete* boundary data, that is given a function u_I (built from measurements) on $I \subset \mathbb{T}$, the inverse problem consists in determining $\sigma \subset \mathbb{D}$ such that the solution u to (1.1) satisfies:

$$u\big|_I = u_I.$$

Such problems have been considered since [16], mainly by iterative methods. Among recent work, we mention [4] and [12]; an extensive bibliography appears in [11]. Complex analytic methods were introduced in [10] as a way of avoiding repeated resolutions of the associated direct problem.

In order to extend the available data u_I to the whole outer boundary $\mathbb{T}$, the Hilbert transform (or harmonic conjugation) allows one to work in the framework of analytic function theory and Hardy spaces, where appropriate approximation techniques will be used. Indeed, thanks to the Cauchy–Riemann equations, there exists a function U analytic in $\mathbb{D} \setminus \sigma$ such that the above solution u satisfies

$$u = \operatorname{Re} U \quad \text{in} \quad \mathbb{D}.$$

Equivalently, there exists a (conjugate harmonic in $\mathbb{D} \setminus \sigma$) function v such that $U = u + iv$ and

$$\frac{\partial u}{\partial n} = \frac{\partial v}{\partial \theta}, \quad \frac{\partial u}{\partial \theta} = -\frac{\partial v}{\partial n} \quad \text{on} \quad \mathbb{T}.$$

Thus, the trace of U at points $\xi = e^{i\theta}$ on I is given here by:

$$U(\xi) = u_I(\xi) + i \int_{\theta_a}^{\theta} \Phi(e^{i\tau}) \, d\tau, \tag{1.3}$$

for some $e^{i\theta_a} \in I$, and is Hölder smooth up to $\mathbb{T}$, see [1]: $U \in C^{1/2}(\mathbb{T})$. Further, it holds that:

$$U(z) = \frac{1}{2i\pi} \int_{\sigma} \frac{[u](\tau)}{z - \tau} \, d\tau + G(z), \qquad \forall z \in \overline{\mathbb{D}} \setminus \sigma, \tag{1.4}$$

for some function $G \in H^{\infty}$ and if $[u]$ denotes the jump of u on σ, which is known to belong to $C^{1/2}(\sigma)$, see [10].

Sources

Another geometrical inverse problem is to determine sources located inside a domain from partially overdetermined data. The case of pointwise dipolar sources is, in particular, related to applications in medical imaging as the inverse electroencephalography issue (EEG), see e.g. [5]. In dimension 2, this raises the following problem [7]:

$$\begin{cases} \Delta u = \sum_{k=1}^{m} p_k \cdot \nabla \delta_{C_k} & \text{in} \quad \mathbb{D}, \\ \dfrac{\partial u}{\partial n} = \Phi & \text{on} \quad \mathbb{T}, \end{cases} \tag{1.5}$$

with $C_k \in \mathbb{D}$, $p_k \in \mathbb{C}$, and for a flux $\Phi \in L^2_{\mathbb{R}}(\mathbb{T})$ which satisfies (1.2).

From additional *incomplete* boundary data u_I on $I \subset \mathbb{T}$, the inverse sources problem consists in determining the number m, the locations $\{C_k\} \subset \mathbb{D}$ and the complex moments $\{p_k\}$ of the sources, such that the solution u to (1.5) satisfies:

$$u\big|_I = u_I.$$

This problem is discussed in [19] which contains an extensive bibliography.

Using harmonic conjugation and (1.3), this also allows one to build the trace on $I \subset \mathbb{T}$ of a function U analytic and Hölder smooth in $\mathbb{D} \setminus \{C_k\}$:

$$U(z) = \frac{1}{2i\pi} \sum_{k=1}^{m} \frac{p_k}{z - C_k} + G(z), \qquad \forall z \in \overline{\mathbb{D}} \setminus \{C_k\}, \tag{1.6}$$

for some function $G \in A(\mathbb{D})$, see [7].

Recovery of analytic function

Let $\mathcal{S}$ denote either the singular integral in expression (1.4) or the sum in (1.6), so that in both cases $U = \mathcal{S} + G$.

Assume that measurements $u_I^\emptyset$ of a solution to (1.1) or (1.5) on a *safe* domain (with $\sigma = \emptyset$) are also available on I, from the same flux Φ. This allows one to obtain on I the associated function $U_\emptyset$, see (1.3):

$$U_\emptyset(\xi) = u_I^\emptyset + i \int_{\theta_a}^{\theta} \Phi(e^{i\tau}) \, d\tau,$$

for some $e^{i\theta_a} \in I$, which is analytic in the whole of $\mathbb{D}$ in view of (1.4) or (1.6), and whose imaginary part coincides with that of U on $\mathbb{T}$. As a result, the function

$$f = U - U_\emptyset = G - U_\emptyset + \mathcal{S} = g + \mathcal{S},$$

with $g = G - U_\emptyset$, is real valued on $\mathbb{T}$. Because $g \in H^2$ while $\mathcal{S} \in \overline{H_0^2}$, we get that

$$\mathcal{S} = \overline{g} \quad \text{on} \quad \mathbb{T},$$

whence

$$f = 2 \operatorname{Re} g = 2 \operatorname{Re} \mathcal{S} \quad \text{on} \quad \mathbb{T}.$$

We therefore seek to recover g, hence also $\mathcal{S}$ and ultimately σ or $\{C_k\}$, from the partial and normally corrupted values of f obtainable on I, where $f = u_I - u_I^\emptyset$. To do this we use the methods of analytic approximation, as outlined in the next section.

2. Bounded extremal problems

2.1. Statement of the problem

A systematic approach (using duality) to extremal problems in Hardy spaces can be traced back to [18, 24] around 1950 and has been extensively studied since then [15, 21]. The standard Bounded Extremal Problem (BEP), which has its origins with Krein and Nudel'man (see [2, 9, 22]), and is of importance in frequency-domain systems identification, may be stated as follows.

Problem 2.1. *Given $f \in L^2(I)$, $\phi \in L^2(J)$ and $M > 0$, find $g_0 \in H^2$ such that $\|g_0 - \phi\|_J \leq M$ and*

$$\|g_0 - f\|_I = \inf \{\|g - f\|_I : g \in H^2, \|g - \phi\|_J \leq M\}.$$

For the application to the inverse problem outlined above, the following version of the problem is more appropriate.

Problem 2.2. *Given $f \in L^2_{\mathbb{R}}(I)$, $\phi \in L^2(J)$ and positive constants α, β, M, let $\phi_r = \operatorname{Re} \phi$ and $\phi_i = \operatorname{Im} \phi$ and define the set $\mathcal{C}_{\alpha,\beta,M}$ by*

$$\mathcal{C}_{\alpha,\beta,M} = \{g \in H^2 : \alpha^2 \|\operatorname{Re} g - \phi_r\|_J^2 + \beta^2 \|\operatorname{Im} g - \phi_i\|_J^2 \leq M^2\}.$$

Find $g_0 \in \mathcal{C}_{\alpha,\beta,M}$ such that

$$\|f - \operatorname{Re} g_0\|_I = \inf \{\|f - \operatorname{Re} g\|_I : g \in \mathcal{C}_{\alpha,\beta,M}\}.$$

Remark 2.3. Ideally, we might prefer to work with a constraint such as $\|\operatorname{Im} g\|_J \leq M$ (small), that is, to take $\alpha = 0$, but the solution to this problem is no longer unique in general. To see this, note that the function $w(z) = \operatorname{arccosh} s$, where $s = i(1-z)/(1+z)$, lies in H^2. This provides a conformal mapping from the region $\{z \in \mathbb{C} : |z| < 1\}$, via $\{s \in \mathbb{C} : \operatorname{Im} s > 0\}$, to the domain

$$\{w \in \mathbb{C} : \operatorname{Re} w > 0, 0 < \operatorname{Im} w < \pi\}.$$

See for example [25, p. 177]. Taking I to be the circular arc $\mathbb{T} \cap \{\operatorname{Re} z \geq 0\}$, we see that $\operatorname{Re} w = 0$ on I, whereas $|\operatorname{Im} w| \leq \pi$ on J. Hence, for $f = \phi_r = \phi_i = 0$, a family of multiples of w solves the extremal problem simultaneously.

We can of course take α small in comparison with β, if we choose. An alternative constraint that would be of interest is $\|\alpha \operatorname{Re} g \pm \beta \operatorname{Im} g\|_J \leq M$, but this is closely related to Problem 2.2 because of the parallelogram identity

$$\|u + v\|^2 + \|u - v\|^2 = 2\|u\|^2 + 2\|v\|^2,$$

which holds in any Hilbert space, in particular in $L^2(J)$. We remark also that taking $\alpha = \beta = 1$ in Problem 2.2 provides the simple norm constraint of Problem 2.1, namely $\|g\|_J \leq M$.

A related problem is the following, which was solved in [20].

Problem 2.4. *Given $f \in L^2(I)$, $\phi \in L^2_{\mathbb{R}}(J)$ and $M \geq 0$, find $g_1 \in H^2$ such that $\|\operatorname{Im} g_1 - \phi\|_J \leq M$ and*

$$\|g_1 - f\|_I = \inf \{\|g - f\|_I : g \in H^2, \|\operatorname{Im} g - \phi\|_J \leq M\}. \tag{2.1}$$

2.2.   A general Hilbert space framework

In fact Problems 2.2 and 2.4 can both be re-expressed using the language of [14], provided that we accept the additional technical difficulty involved in regarding H^2 as a Hilbert space with *real* scalars. To see this, we recall the following result. It was stated originally for complex Hilbert spaces, because the main application was in the construction of invariant subspaces, but this is not necessary.

Let $\mathcal{H}$, $\mathcal{I}$ and $\mathcal{J}$ be real Hilbert spaces and $A : \mathcal{H} \to \mathcal{I}$ and $B : \mathcal{H} \to \mathcal{J}$ bounded linear operators, such that A and B are coprime, in the sense that there exists a constant $\eta > 0$ such that

$$\|Ax\|^2 + \|Bx\|^2 \geq \eta\|x\|^2 \qquad \text{for all} \quad x \in \mathcal{H}. \tag{2.2}$$

We suppose also that A has dense range. Then the associated extremal problem is as follows.

Problem 2.5. *Given $x_{\mathcal{J}} \in \mathcal{J}$, $x_{\mathcal{I}} \in \mathcal{I}$, and $M > 0$, let $\mathcal{C}_{x_0}^M$ be defined by*

$$\mathcal{C}_{x_0}^M = \{y \in \mathcal{H} : \|By - x_{\mathcal{J}}\| \leq M\},$$

and suppose that $\mathcal{C}_{x_0}^M$ is nonempty whereas $Ay \neq x_{\mathcal{I}}$ for all $y \in \mathcal{C}_{x_0}^M$. Find $y_0 \in \mathcal{C}_{x_0}^M$ such that

$$\|Ay_0 - x_{\mathcal{I}}\| = \inf\{\|Ay - x_{\mathcal{I}}\| : y \in \mathcal{C}_{x_0}^M\}. \tag{2.3}$$

Under the hypotheses above, Problem 2.5 has a unique solution and the extremal vector saturates the constraint, in the sense that $\|By_0 - x_{\mathcal{J}}\| = M$.

Theorem 2.6 ([14]). *The solution to Problem 2.5 is given by $(A^*A - \gamma B^*B)y_0 = A^*x_{\mathcal{I}} - \gamma B^*x_{\mathcal{J}}$, where $\gamma < 0$ is the unique constant such that $\|By_0 - x_{\mathcal{J}}\| = M$.*

We shall discuss in Section 3 how to determine the appropriate value of the parameter γ, using the fact that the relation between M and γ is continuous and monotonic.

In practical applications, $x_{\mathcal{I}}$ represents measured data, $x_{\mathcal{J}}$ is a reference vector, and M a constraint that may be chosen in the light of experience. It is therefore essential to know that the model obtained, which is here denoted y_0, will depend continuously on the data, and this is shown in the next result. Recall that we assumed in Problem 2.5 that $x_{\mathcal{I}} \notin A\mathcal{C}_{x_0}^M$.

Theorem 2.7. *The solution y_0 to Problem 2.5 depends continuously on $x_{\mathcal{I}}$ and M, $x_{\mathcal{J}}$ being fixed.*

Proof. First, for a fixed $x_{\mathcal{I}}$, the quantity $e = \|Ay_0 - x_{\mathcal{I}}\|$ is a convex decreasing function of M, since we can take linear combinations of solutions for different M; hence e varies continuously with M.

Now suppose that $\|x_{\mathcal{I}}^{(n)} - x_{\mathcal{I}}\| \to 0$ and $M_n \to M$. We claim that the corresponding solutions $y_0^{(n)}$ converge in norm to y_0. Note first that $e^{(n)} \to e = e(M)$, for if $\delta > 0$

and $e^{(n)} < e - \delta$ infinitely often, then $\|Ay_0^{(n)} - x_{\mathcal{I}}\| < e - \delta/2$ infinitely often and $\|By_0^{(n)} - x_{\mathcal{J}}\| = M_n$, so $e(M_n) < e(M) - \delta/2$, a contradiction to the continuity of e with respect to M. Or if $e^{(n)} > e + \delta$ infinitely often, let $\tilde{y}_0^{(n)}$ denote the solution associated with $x_{\mathcal{J}}, x_{\mathcal{I}}$ and M_n. Then, using the above continuity property of e with respect to M, we get that $\|A\tilde{y}_0^{(n)} - x_{\mathcal{I}}\| \to e$, whence $\|A\tilde{y}_0^{(n)} - x_{\mathcal{I}}\| < e^{(n)}$ infinitely often, a contradiction to the optimality of $y_0^{(n)}$. We deduce that $e^{(n)} \to e$.

Now $(y_0^{(n)})$ is a bounded sequence. We show that every subsequence of it has a further sub-subsequence converging in norm to y_0; this will imply that the original sequence also converges in norm to y_0. Now suppose by passing to a subsequence and relabelling that $y_0^{(n)}$ converges weakly to y'; then

$$\begin{pmatrix} A \\ B \end{pmatrix} y_0^{(n)} \text{ converges weakly to } \begin{pmatrix} A \\ B \end{pmatrix} y',$$

and it follows that $\|Ay' - x_{\mathcal{I}}\| \le e$ and $\|By' - x_{\mathcal{J}}\| \le M$, hence $y' = y_0$. Also $\|Ay_0^{(n)} - x_{\mathcal{I}}\| \to \|Ay_0 - x_{\mathcal{I}}\|$ and $\|By_0^{(n)} - x_{\mathcal{J}}\| \to \|By_0 - x_{\mathcal{J}}\|$, implying that $Ay_0^{(n)} \to Ay_0$ and similarly $By_0^{(n)} \to By_0$. Hence $\|y_0^{(n)} - y_0\| \to 0$. The result follows. $\quad\square$

The following result enables one to find an appropriate parameter in Theorem 2.6 (and this will be used again in Corollary 2.9) by an interval-halving search.

Proposition 2.8. *In Theorem 2.6, the parameter M depends continuously and monotonically on γ, and vice-versa.*

Proof. Since $(A^*A - \gamma B^*B)^{-1}$ depends continuously on γ for $\gamma < 0$, we see that y_0, and hence M also, depends continuously on γ. It is impossible for two different values of γ to yield the same y_0, as otherwise we would have $B^*By_0 = B^*x_{\mathcal{J}}$, implying that the same y_0 is a solution to Problem 2.5 for *every* value of γ, which is clearly impossible. Thus the mapping from γ to M is continuous and also monotonic (since injective), and hence the same is true of its inverse. $\quad\square$

2.3. Solution to Problem 2.2

Back to Problem 2.2, let us now take $\mathcal{H} = H^2$, $\mathcal{I} = L^2_{\mathbb{R}}(I)$, and $\mathcal{J} = L^2_{\mathbb{R}}(J) \oplus L^2_{\mathbb{R}}(J)$ (the L^2 direct sum), all regarded as *real* Hilbert spaces. The real inner product on H^2 is just $\mathrm{Re}\langle h_1, h_2 \rangle$, where $\langle h_1, h_2 \rangle$ is the usual inner product. The real-linear operators A and B are defined by

$$Ag = (\mathrm{Re}\, g)\big|_I, \qquad Bg = (\alpha \, \mathrm{Re}\, g, \beta \, \mathrm{Im}\, g)\big|_J,$$

for $g \in \mathcal{H}$. Moreover, $x_{\mathcal{J}} = (\alpha \phi_r, \beta \phi_i)$ and $x_{\mathcal{I}} = f$. The desired solution y_0 is the same as our g_0.

To see that condition (2.2) is satisfied we may use the theorem of M. Riesz that the Hilbert transform is a contraction, as in Lemma 3 of [20] where it is shown that there

is an absolute constant $C > 0$ such that, for all $h \in H^2$, one has

$$\|h\| \leq C \max\{\|h\|_I, \|\operatorname{Im} h\|_J\}.$$

On exchanging the roles of I and J, and replacing h by ih, one arrives easily at an inequality equivalent to (2.2).

The adjoint operators $A^* : \mathcal{I} \to \mathcal{H}$ and $B^* : \mathcal{J} \to \mathcal{H}$ are given by

$$A^* f = P(f \vee 0), \qquad B^*(\phi_1, \phi_2) = P(0 \vee (\alpha \phi_1 + i\beta \phi_2)).$$

Corollary 2.9. *The solution to Problem 2.2 is given by*

$$P(\operatorname{Re} g_0 \chi_I - \gamma(\alpha^2 \operatorname{Re} g_0 + i\beta^2 \operatorname{Im} g_0)\chi_J) = P(f\chi_I - \gamma(\alpha^2 \phi_r + i\beta^2 \phi_i)\chi_J), \quad (2.4)$$

where $\gamma < 0$ is the unique constant such that $\alpha^2 \|\operatorname{Re} g_0 - \phi_r\|_J^2 + \beta^2 \|\operatorname{Im} g_0 - \phi_i\|_J^2 = M^2$.

Proof. This is now a simple consequence of Theorem 2.6, using the identifications above. $\qquad\square$

Let $T : H^2 \to H^2$ be the Toeplitz operator defined by

$$Tg = P\chi_J\, g.$$

Introduce the Hankel operator $H : H^2 \to \overline{H}^2$ defined by

$$Hg = \overline{P}\chi_J\, g.$$

Put

$$\lambda = 1 + \gamma\alpha^2 < 1, \qquad \mu = \gamma\beta^2 < 0. \tag{2.5}$$

Define

$$\Gamma g = g + g(0) - (\lambda + \mu)Tg - (\lambda - \mu)\overline{Hg},$$

for $g \in H^2$ (observe that $\overline{Hg} = \overline{\overline{P}\chi_J\, g} = P\chi_J\, \bar{g}$). Write

$$F = 2P(f\chi_I - \gamma(\alpha^2 \phi_r + i\beta^2 \phi_i)\chi_J).$$

It can be deduced from (2.4) that

$$\Gamma g_0 = F.$$

For $g \in H^2$, let $\hat{g} \in l_{\mathbb{N}}^2(\mathbb{C})$ denote the sequence of its Fourier coefficients. Introduce now the linear operators T_F and H_F on $l_{\mathbb{N}}^2(\mathbb{C})$ defined by:

$$T_F\, \hat{g} = \widehat{Tg}, \qquad \overline{H_F\, \hat{g}} = \widehat{\overline{Hg}}.$$

It follows that, with $e_0 = (1, 0, \dots) \in l_{\mathbb{N}}^2(\mathbb{C})$:

$$\widehat{\Gamma g} = \hat{g} + \hat{g}(0)e_0 - (\lambda + \mu)T_F\, \hat{g} - (\lambda - \mu)\overline{H_F\, \hat{g}}. \tag{2.6}$$

This allows us to write:

$$\widehat{\Gamma g} = \Gamma_r \operatorname{Re} \hat{g} + i\Gamma_i \operatorname{Im} \hat{g},$$

where Γ_r and Γ_i are real linear operators on real sequences in $l^2_{\mathbb{N}}(\mathbb{R})$.

Taking real and imaginary parts in (2.6) leads to:

$$\Gamma_r a = a + a(0)e_0 - (\lambda + \mu)T_F\,a - (\lambda - \mu)H_F\,a, \qquad (2.7)$$

$$\Gamma_i a = a + a(0)e_0 - (\lambda + \mu)T_F\,a + (\lambda - \mu)H_F\,a, \qquad (2.8)$$

for $a \in l^2_{\mathbb{N}}(\mathbb{R})$. Then

$$\operatorname{Re} \hat{g}_0 = \Gamma_r^{-1} \operatorname{Re} \hat{F}, \qquad \operatorname{Im} \hat{g}_0 = \Gamma_i^{-1} \operatorname{Im} \hat{F}. \qquad (2.9)$$

2.4. More on Problem 2.4

For Problem 2.4, we take $\mathcal{H} = H^2$, $\mathcal{I} = L^2(I)$, $\mathcal{J} = L^2_{\mathbb{R}}(J)$, and use the real-linear operators A and B defined by

$$Ag = g\big|_I, \qquad Bg = (\operatorname{Im} g)\big|_J.$$

In [20], it was conjectured that the analogous problem for L^∞ and H^∞ might be ill-posed. This is in fact the case, as the following example shows.

Example 2.10. Let I be the arc $\{z \in \mathbb{T} : |\arg z| \leq \pi/4\}$, and $J = \mathbb{T} \setminus I$ as usual. Define $f(z) = \log\left((1 - iz)/(1 + iz)\right)$, where we take analytic continuation from the branch of log with $f(0) = \log 1 = 0$. This function has the following properties:

Since $z \mapsto (1-iz)/(1+iz)$ is a conformal bijection between the disc $\mathbb{D}$ and the right half plane $\mathbb{C}_+$, and $\log\left(re^{i\theta}\right) = \log r + i\theta$, we see that $|\operatorname{Im} f| \leq \pi/2$ on $\mathbb{T}$, whereas f is unbounded. Indeed f is in H^2 but not H^∞. However, f is bounded on I.

Now take $M = \pi/2$ and $\phi = 0$. We claim that

$$\inf\{\|g - f\|_{L^\infty(I)} : g \in H^\infty,\ \|\operatorname{Im} g - \phi\|_{L^\infty(J)} \leq M\} = 0.$$

For if we write $f = u + iv$ (real and imaginary parts), then f can be approximated arbitrarily closely on I by the Fejér means $g_n = u_n + iv_n$ of its Fourier series, which in this case are just polynomials in z. This follows because f is continuous on I and $f \in L^1(\mathbb{T})$. Moreover, v_n is just the Fejér mean of the Fourier series for v, and, by well-known properties of the Fejér kernel [26, p. 86], $\|v_n\|_\infty \leq \|v\|_\infty = \pi/2$.

On the other hand, it is clear that there is no function $g \in H^\infty$ such that $g = f$ in I, since I is a set of uniqueness for H^2.

3. Algorithmic and numerical results

3.1. An algorithm for Problem 2.2

A `matlab` version of the described algorithm (Section 2.3) has been implemented. Analytic functions, as well as Hankel and Toeplitz operators, are approximated on

the Fourier basis, keeping only a finite number N of Fourier coefficients. In all the following examples, $N = 512$.

Searching for the good value of γ is done iteratively: starting with an initial prediction $\gamma = \gamma_0$, we compute the analytic function $g_0 = g_0(\gamma)$ given by equations (2.9) together with (2.5), (2.7), (2.8).

We then decide to increase or decrease γ according to the value of[1]

$$e_J(\gamma) = \alpha^2 \|\operatorname{Re} g_0(\gamma) - \phi_r\|_J^2 + \beta^2 \|\operatorname{Im} g_0(\gamma) - \phi_i\|_J^2 :$$

$$\text{if} \quad e_J(\gamma) > M^2 \quad \text{then increase} \quad \gamma,$$

$$\text{if} \quad e_J(\gamma) < M^2 \quad \text{then decrease} \quad \gamma.$$

Convergence is guaranteed in view of the continuous monotonic relation between γ and M established in Proposition 2.8.

In fact, without further information, the choice of the control parameter M is likely to be heuristic; however, an unsuitable choice would be reflected in an unreasonable error achieved in the approximation problem. A slight modification of the preceding algorithm has been implemented, allowing one to control a dimensionless parameter k which is the ratio of the error $e_J(\gamma)$ on J introduced above to the approximation error on I: $e_I(\gamma) = \|g_0(\gamma) - f\|_I^2$. These two quantities vary in a monotonic opposite way when γ varies, and the final value for γ is found by an interval-halving procedure. Then, for a given k, the actual minimization problem is: $\min_\gamma \{e_I(\gamma) \mid e_J(\gamma) - k e_I(\gamma) < 0\}$. Good values for k lie in a neighbourhood of 1, typically $k \in [1/10, 10]$, which means that the errors on I and J have *the same order of magnitude*.

3.2. Inverse problem examples

The following examples show results for

- the crack inverse problem with partial boundary data (Examples 1 and 2),
- the dipolar sources inverse problem with partial boundary data (Examples 3 and 4),

as described in Section 1.2. There are actually two issues here: first, recovery of missing boundary data, which is achieved by the resolution of Problem 2.2; second, more ambitiously, attempting to find the approximate location of the singularities, which is done by best L^2 rational approximation methods that are justified elsewhere [6, 8, 17]. Pretty good "recovery" capacity of the combined algorithm is demonstrated by these examples. Note that Theorem 2.7 guarantees the robustness of the first step with respect to available (possibly noisy) data, while strong continuity properties of the second step are established in [6].

3.2.1 Cracks

For crack examples, we apply the following procedure. First we solve the "direct problem": the 2D domain is the unit disk $\mathbb{D}$. Cracks are modelled by thin subdomains.

---

[1]To be more precise, γ is allowed to vary in the interval $(-\infty, 0]$. Instead, we map this interval to the bounded interval $[0, 1]$ by putting $\gamma = r/(r - 1)$, and we look for the appropriate value of $r \in [0, 1]$.

Given a boundary flux Φ satisfying the zero-mean value property, the Neumann problem defined by (1.1) is solved for the zero-mean solution u. For this we use a PDE integration library[2]. The same equations with same boundary flux Φ are solved on a safe (no crack) domain and this gives the zero-mean value solution $u^\emptyset$. Boundary values of the error function $u - u^\emptyset$ are picked on the I subarc and used as "measures".

Then, we solve the "inverse problem" of finding the missing imaginary part on subarc I and the missing data on subarc J of the error function. This is done by solving for the analytic function g of Section 1.2, a solution to Problem 2.2. We take $f = u - u^\emptyset$ on I and we choose as reference constraint function $\phi = 0$ on J. Finally, a best L^2 rational approximation of the conjugate $\overline{g}$ of the analytic extension g is performed [17]. The computed poles are seen to accumulate on geodesic arcs, which are arcs of circles orthogonal to the boundary $\mathbb{T}$, as expected for piecewise analytic cracks; see [8, 11] where the result is established for an analytic crack. Of course, in general the crack is not a geodesic arc, but there is such an arc which joins the endpoints of the crack (or the endpoints of its analytic parts), and this assists in locating the crack.

In Examples 1 and 2 of Section 3.3, we identify cracks. The flux is chosen to be a trigonometric polynomial of low degree $\Phi(x, y) = x$. The solution g of the inverse problem for $f = u - u^\emptyset$ is seen in the first plot of Figures 2 and 4, respectively. We note that it is virtually indistinguishable from the data, where the latter is given. For the subsequent rational approximation step, the number of poles of the approximant is decided according to the L^2 error observed.

In both examples, significant poles accumulate near the geodesic passing through the extremities of the crack. The supposed unknown crack is drawn for comparison (heavy line). A number of poles also accumulate on arcs of circles joining the endpoints of I and J. However, their residues are small and they are a result of the first approximation step, which induces a discontinuity of g at these points. This is linked to the choice of M and an alternative approach would be to work with other constraints, such as those given by Hardy–Sobolev or uniform norms.

3.2.2 Dipoles

For dipole examples, we apply the following procedure. We solve the "direct problem" in $\mathbb{D}$: the fundamental solution E (null at infinity) of the dipole distribution is explicitly given ($E = \operatorname{Re} \mathcal{S}$, see equation 1.6) and we compute a harmonic function h so that the solution $u = h + E$ has normal derivative on $\mathbb{T}$ equal to Φ.

Here we take again $\phi = 0$ as constraint reference on J, so that $u^\emptyset = 0$ and $f = u$ on I. Then, we solve the "inverse problem" by solving Problem 2, just as for cracks, thus getting g, shown in the second plot of Figures 5 and 7, for Examples 3 and 4 of Section 3.3. Again it matches the given data very well, where the latter is available.

Once more, in the subsequent rational approximation step, the number of poles of the approximant is decided according to the L^2 error observed. The most significant poles of the best L^2 rational approximant to $\overline{g}$ are seen to be located at the true dipoles, as established in [7]. This is a direct consequence of the fact that $\mathcal{S}$ is rational. (Note that in [7] the case of monopolar sources is also considered, which gives rise to a

---

[2]The `matlab R13 pde toolbox`

function S with logarithmic singularities; in this case the poles would accumulate in a manner similar to that in the situation of a crack, as described above.) The remaining poles accumulate on an arc of circle orthogonal to the boundary $\mathbb{T}$, containing the endpoints of the subarcs I and J. However, once again these additional poles have residues much smaller than the others, which are located near the true sources.

3.3. Numerical results

We present the results of some numerical experiments: in each case, for reasons of space, we demonstrate the results obtained with a single choice of Φ. Clearly, further choices would help in locating the singularities in question. There is, however, an issue of identifiability here: for example, it is necessary that the cracks do not lie along the level lines of the associated solution.

Example 1. This example shows how the data extend analytically, and how rational approximation can help to locate the crack as previously explained (Section 3.2.1).

Problem 2.2 is solved with a subarc I corresponding to $[\pi/6, 11\pi/6]$ and with $f = u - u^\emptyset$ and $\phi = 0$. The values $\alpha = 0.01$, $\beta = 1$ of the numerical parameters give rise to the errors $e_I = \|f - \operatorname{Re} g_0\|_I = 2.8e{-}2$ on I and $e_J = M = 6e{-}2$ on J.

Example 2. In this example, the boundary data $f = u - u^\emptyset$ (still with $\phi = 0$) are additionally corrupted by an additive noise (signal/noise = 20), and the I subarc where data are measured is only $[\pi/3, 5\pi/3]$. The error values are then $e_I = 0.65e{-}2$ on I and $e_J = 1.5e{-}2$ on J. We can see that the poles of the rational approximant still help to locate the crack.

Example 3. This example illustrates how one can locate positions and estimate moments of 2 dipolar sources, as described in Section 3.2.2 Data $f = u$ (and $\phi = 0$ whence $u^\emptyset = 0$) of the inverse problem are picked within the subarcs $I = [\pi/4, 7\pi/4]$ and $[\pi/3, 5\pi/3]$ where we solve for Problem 2.2. Resulting errors are $e_I = 0.21$ on I and $e_J = 0.45$ on J. The first poles ($n = 2$, and 8) of the rational approximant are shown with their corresponding residue.
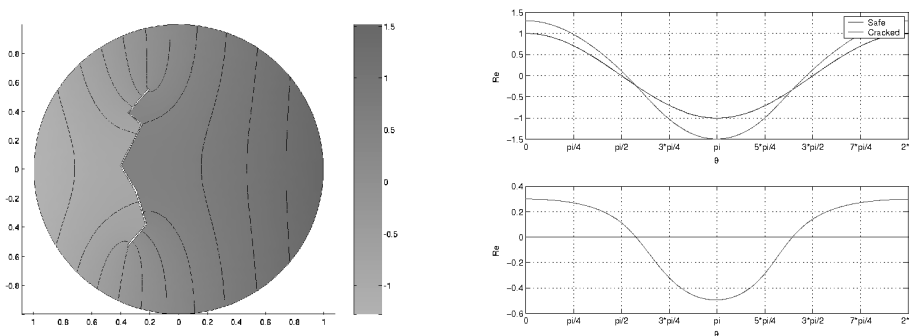
Figure 1. Example 1. Direct problem: domain with level curves for u, boundary solutions u and $u^\emptyset$, and error function $u - u^\emptyset$
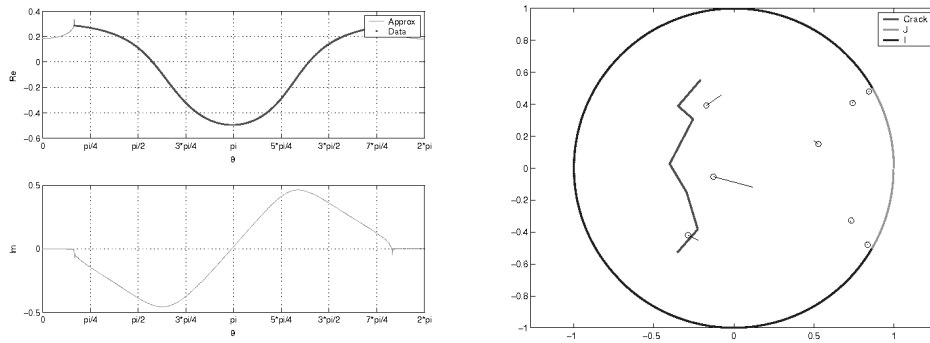
Figure 2. Example 1. Inverse problem: analytic extension g, $I = [\pi/6, 11\pi/6]$ and poles of the rational approximant of $\overline{g}$, $n = 8$
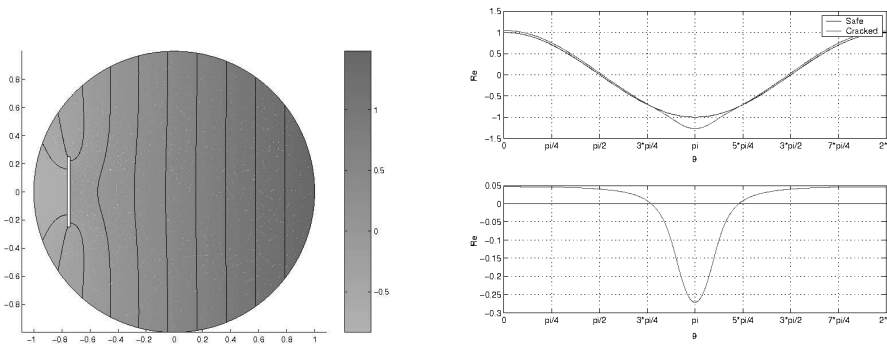
Figure 3. Example 2. Direct problem: domain with level curves for u, boundary solutions u and $u^{\emptyset}$, and error function $u - u^{\emptyset}$
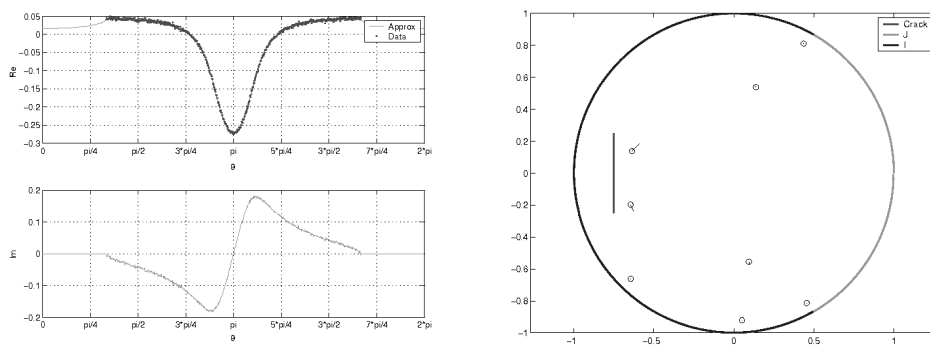
Figure 4. Example 2. Inverse problem: analytic extension g, $I = [\pi/3, 5\pi/3]$ and poles of the rational approximant of $\overline{g}$, $n = 8$
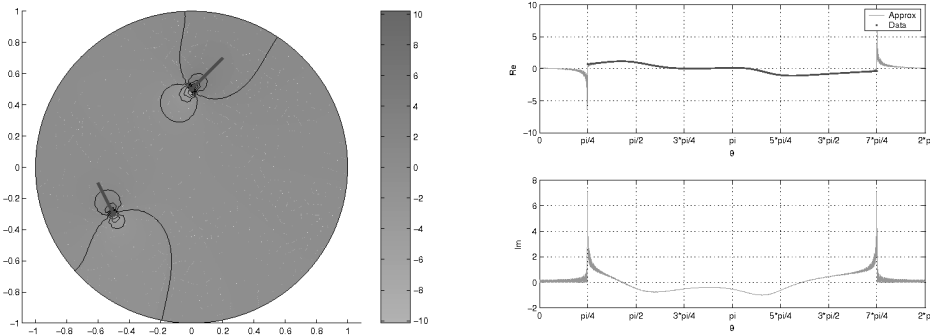
Figure 5. Example 3. Domain with level curves for u (direct problem); analytic extension g of boundary solution, $I = [\pi/4, 7\pi/4]$
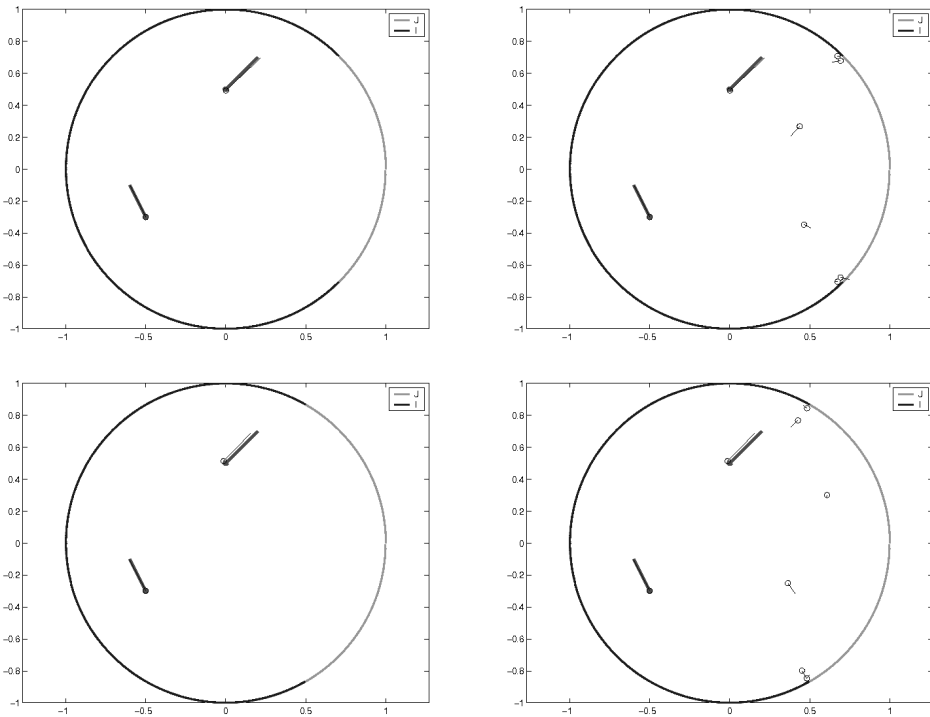
Figure 6. Example 3. Inverse problem: $I = [\pi/4, 7\pi/4]$, and $[\pi/3, 5\pi/3]$, poles of the rational approximant of $\overline{g}$, $n = 2$, and 8
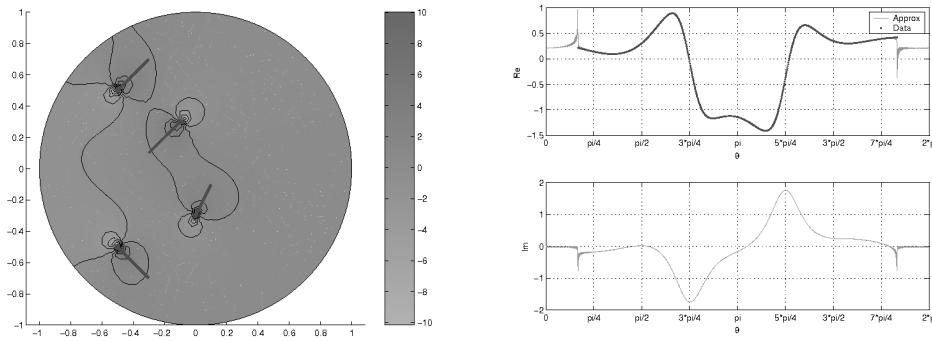
Figure 7. Example 4. Domain with level curves for u (direct problem); analytic extension g of boundary solution, $I = [\pi/6, 11\pi/6]$
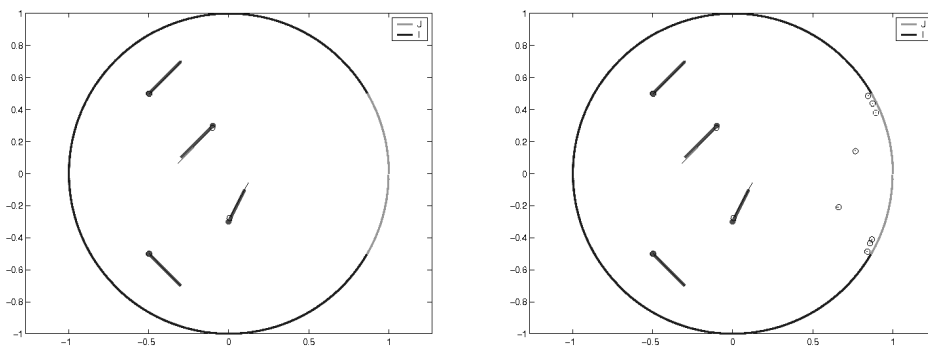
Figure 8. Example 4. Inverse problem: $I = [\pi/6, 11\pi/6]$, poles of the rational approximant of $\overline{g}$, $n = 4$, and 12

Example 4. This example illustrates the case of 4 dipolar sources. Data $f = u$ ($\phi = 0$, $u^\emptyset = 0$) of the inverse problem are picked within the subarc $I = [\pi/6, 11\pi/6]$ where Problem 2.2 is solved, with errors $e_I = 3e{-}2$ on I and $e_J = 7e{-}2$ on J. The first poles ($n = 4$, and 12) of the rational approximant are shown with their corresponding residue.

4. Conclusions

We have seen that the methods of constrained approximation provide a numerically efficient technique for certain inverse diffusion problems on the disc, by the strategy of recovering an analytic function from measurements of its real part on a subset of the circle. By means of a conformal equivalence it is possible to perform analogous calculations in other simply-connected two-dimensional domains.

Although we have established a significant stability result (Theorem 2.7) showing the robustness of the solution with respect to the given data, it remains open whether one has continuity of the solution y_0 given by Theorem 2.6, when all of $x_{\mathcal{J}}$, $x_{\mathcal{I}}$ and M are allowed to vary simultaneously.

An extension of some of the ideas of this paper to multiply-connected domains, such as the annulus, is a topic of current investigation [23]: it requires additional tools, such as the notion of a harmonic conjugate in a non-simply connected region, and the analysis of the Hardy spaces of an annulus.

References

1. A. Ben Abda, M. Kallel, J. Leblond, and J.-P. Marmorat, Line-segment cracks recovery from incomplete boundary data. *Inverse Problems* **18** (2002), 1057–1077.

2. D. Alpay, L. Baratchart, and J. Leblond, Some extremal problems linked with identification from partial frequency data. In: *Analysis and Optimization of Systems: State and Frequency Domain Approaches for Infinite-Dimensional Systems (Sophia-Antipolis, 1992)*. Springer, Berlin, 1993, 563–573.

3. M. Andersson, *Topics in Complex Analysis*. Springer-Verlag, 1997.

4. S. Andrieux and A. Ben Abda, Identification of planar cracks by complete overdetermined data: inversion formulae. *Inverse Problems* **12** (1996), 553–563.

5. A. El Badia and T. Ha-Duong, An inverse source problem in potential analysis. *Inverse Problems* **16** (2000), 651–663.

6. L. Baratchart, Existence and generic properties of L^2 approximants for linear systems. *IMA J. of Mathematical Control and Information* **3** (1986), 89–101.

7. L. Baratchart, A. Ben Abda, F. Ben Hassen, and J. Leblond, Pointwise sources recovery and approximation. *Inverse problems* (2005), 51–74.

8. L. Baratchart, R. Küstner, and V. Totik, Zero distributions via orthogonality. *Ann. Inst. Fourier (Grenoble)* **55** (2005), 1455–1499.

9. L. Baratchart and J. Leblond, Hardy approximation to L^p functions on subsets of the circle with $1 \leq p < \infty$. *Constr. Approx.* **14** (1998), 41–56.

10. L. Baratchart, J. Leblond, F. Mandréa, and E. B. Saff, How can meromorphic approximation help solve some 2D inverse problems for the Laplacian?. *Inverse problems* **15** (1999), 79–90.

11. L. Baratchart, F. Mandréa, E. Saff, and F. Wielonsky, 2D inverse problems for the Laplacian: a meromorphic approximation approach. *J. Math. Pures et Appl.* **86**, 1 (2006), 1–41.

12. M. Brühl, M. Hanke, and M. Pidcock, Crack detection using electrostatic measurements. *M2AN Math. Model. Numer. Anal.* **35** (2001), 595–605.

13. I. Chalendar, J. Leblond, and J. R. Partington, Approximation problems in some holomorphic spaces, with applications. In: *Systems, Approximation, Singular Integral Operators, and Related Topics, Proceedings of IWOTA 2000*. Birkhäuser, 2001, 143–168.

14. I. Chalendar and J. R. Partington, Constrained approximation and invariant subspaces. *J. Math. Anal. Appl.* **280** (2003), 176–187.

15. P. L. Duren, *Theory of H^p Spaces*. Academic Press, New York, 1970.

16. A. Friedman and M. Vogelius, Determining cracks by boundary measurements. *Indiana Univ. Math. J.* **38** (1989), 527–556.

17. P. Fulcheri and M. Olivi, Matrix rational H^2-approximation: a gradient algorithm based on Schur analysis. *SIAM J. on Control & Optim.* **36** (1998), 2103–2127.

18. S. Ya. Havinson, On some extremal problems of the theory of analytic functions. *Moskov. Gos. Univ. Učenye Zapiski Matematika* **148**, 4 (1951), 133–143 (in Russian); *AMS Translations* **32** (1951), 139–154.

19. V. Isakov, *Inverse Source Problems*. AMS, Providence, 1990.

20. B. Jacob, J. Leblond, J.-P. Marmorat, and J. R. Partington, A constrained approximation problem arising in parameter identification. *Linear Algebra and its Applications* **351/352** (2002), 487–500.

21. S. Ya. Khavinson, *Two Papers on Extremal Problems in Complex Analysis*. AMS, 1986.

22. M. G. Kreĭn and P. Ja. Nudel'man, Approximation of functions in $L_2(\omega_1, \omega_2)$ by transmission functions of linear systems with minimal energy. *Problemy Peredači Informacii* **11** (1975), 37–60. English translation.

23. J. Leblond, M. Mahjoub, and J. R. Partington, Analytic extensions and Cauchy-type inverse problems on annular domains: stability results. *J. Inv. Ill-Posed Problems* **14** (2006), 189–204.

24. A. J. Macintyre and W. W. Rogosinski, Extremum problems in the theory of analytic functions. *Acta Math.* **82** (1950), 275–325.

25. H. A. Priestley, *Introduction to Complex Analysis*. Oxford University Press, New York, 1990. 2nd ed.

26. A. Zygmund, *Trigonometric Series*. Cambridge University Press, 1988. 2nd ed.

Author information

J. Leblond, INRIA, BP 93, 06902 Sophia-Antipolis Cedex, France.
Email: leblond@sophia.inria.fr

J.-P. Marmorat, CMA-EMP, BP 93, 06902 Sophia-Antipolis Cedex, France.
Email: jean-paul.marmorat@ensmp.fr

J. R. Partington, School of Mathematics, University of Leeds, Leeds LS2 9JT, U.K..
Email: J.R.Partington@leeds.ac.uk